International Journal of Wavelets, Multiresolution
and Information Processing
(2019) 1941021 (25 pages)
© World Scientific Publishing Company
DOI: 10.1142/S0219691319410212

Int. J. Wavelets Multiresolut Inf. Process. Downloaded from www.worldscientific.com
by UNIVERSITY OF NEW ENGLAND on 01/01/20. Re-use and distribution is strictly not permitted, except for Open Access articles.

A Unified Power Quality Conditioner for Power Quality Improvement in Distributed Generation Network Using Adaptive Distributed Power Balanced Control (ADPBC)

M. R. Mohanraj
Department of EEE, Excel College of Engineering and Technology
Nammakal, Tamil Nadu, India
mohanrajeee89@yahoo.com

R. Prakash
Department of EEE, Vivekananda College of Engineering for Women
Tiruchengode, Tamil Nadu, India
prakash01EEE@yahoo.com

Received 29 March 2019
Revised 16 April 2019
Accepted 9 May 2019
Published 2 August 2019

Power quality improvement is one of the central and critical needs in all types of power-driven industries for perfect utilization of sources. However, fundamental inconveniences in power quality have been recognized, for instance, sags, swells, harmonic distortions and different blocks. Among those, sags and swells are overwhelmingly uncovered, and each influences the electrical gadgets or electrical machines and this requires to be compensated with an advancement to ensure any mal-operation or disappointment. To settle these troubles, custom power gadgets are used like unified power quality conditioner (UPQC), dynamic voltage restorer (DVR) and Distributed Static Compensator (DSTATCOM). This work aims to update the power quality in both single-phase and three-phase system using UPQC. The capacity of UPQC to mitigate voltage sag, voltage swell, responsive power remuneration, load balancing, zero voltage direction, and power factor redress and Total Harmonics Distortion (THD) in the appropriation framework is done by utilizing adaptive distributed power balanced control (ADPBC) method. This investigation works on the single-phase UPQC design to utilize two H-connect setups with eight switches and the three-phase UPQC arrangement to use four legs and three-phase four wire course of action. The overall function of the UPQC with distributed generation (DG) system will be able to compensate for the offset voltage and current disturbances with all the compensated data being collected and verified in Internet of Things (IoT) based on conditional Random Fields (CRFs).

Keywords: Power quality; UPQC; total harmonic distortion; adaptive distributed power balanced control.

AMS Subject Classification 2010: 68T05, 68M11, 68W15, 00A71, 00A72, 03C95, 11D04, 18B15, 28A10, 28A20, 32A50, 34A30, 37M05, 60K10, 93B05, 93C65, 93D25, 93E11, 94C30

Int. J. Wavelets Multiresolut Inf. Process. Downloaded from www.worldscientific.com
by UNIVERSITY OF NEW ENGLAND on 01/01/20. Re-use and distribution is strictly not permitted, except for Open Access articles.

1. Introduction

The electrical power system power electronics devices play an essential role in distribution system, which has three aspects, first one is that it introduces valuable industrial and domestic equipment, the second one is that it creates problems, the third one is that it helps to solve problems. Nowadays, modern semiconductor switching devices such as controlled rectifiers, Uninterruptible Power Supplies (UPS), arc furnaces, etc. are widely used mainly in domestic and industrial loads. These nonlinear loads create power quality problems, such as voltage sag, voltage swell, voltage interruption, voltage flickers, voltage spikes, harmonics, etc. These nonlinear loads include voltage Flickers, Voltage interruption, voltage sag, Voltage swell, Voltage spikes, harmonics and their ability to create power quality problem in distribution system. Such poor power quality causes an increase in power losses and other remarkable abnormalities in distribution sides. Thus, it is essential to maintain a high standard of power quality. Earlier, passive filters were used to solve power quality problems. However, because of some limitations of passive filters, nowadays custom power devices are used to explain power quality problems in distribution side. Optional abilities include compensating for active filtering devices, used for load balancing, power factor improvement and voltage regulation.

There are three types of custom power devices, Distribution Static Compensator (DSTATCOM), Dynamic Voltage Restorer (DVR) and Unified Power Quality Conditioner (UPQC). UPQC is one of the devices with custom capability, that has the capability to solve the voltage and current-related problem. It is connected to the load before the load voltage distortion is free. At the same time, the current drawn from the source has to be compensated in a similar way the main constraint being the source current should be in phase with a supply voltage. The interest in Distributed Generation (DG) has increased rapidly. The worldwide concern about environmental pollution and energy shortage has led to the increasing interest in the generation of renewable electrical energy. DG plays a significant role in power system and helps to solve many problems found in a conventional power system.

There are several DGs, such as PV system, fuel cell and wind turbine. Wind power has become the fastest growing energy source among various renewable energy sources. This work deals with the combined operation of UPQC with wind energy and output of DG, the system is connected to DC bus of UPQC. The UPQC with DG helps to compensate Voltage and current power quality problems and gives additional benefits by providing the power to load whenever voltage interruption occurs with source side. This work discusses the combined operation of UPQC with DG, and this system is integrated with wind energy. The proposed method can compensate voltage sag/swell, load current disturbances. In addition to this, it can offset voltage interruption and active power transfer to load and source in both interconnected and is landing mode and help to improve power quality. The combined operation of UPQC with DG is explained. This system is composed of the continuous shunt and series inverter, and the DC connection is attached

Int. J. Wavelets Multiresolut Inf. Process. Downloaded from www.worldscientific.com
by UNIVERSITY OF NEW ENGLAND on 01/01/20. Re-use and distribution is strictly not permitted, except for Open Access articles.

through the wind power system with a rectifier. The proposed system can compensate voltage sag, voltage swell, voltage interruption and current harmonics in interconnected and islanding mode. The proposed systems, are in interconnected and islanding mode which can compensate the interruption of voltage and current, voltage sag, voltage swell, etc. Therefore, the proposed method increases the power quality at the installation in the power distribution system or industrial power systems.

2. Literature Survey

In this method, the total power handled by UPQC is lesser than the other conventional methods. Power quality problems arise due to increased use of the nonlinear power electronic loads, the faults in a distribution network, the starting and stopping of heavy loads. The UPQC is used instead of conventional 12 switch power conditioner which reduces the switching stress, commutation, losses and cost.[2,18,25] Isolated Distributed Generating System Using DSTATCOM, a three-leg voltage source converter (VSC)-based static distribution compensator, is implemented using an adaptive neural network-based control algorithm for harmonics suppression, load balancing and voltage regulation in three-phase three-wire system with a battery energy storage system.[18] The UPQC is one of the significant custom power solutions, which is capable of reducing the supply voltage sublimation effect or static link point at the end of the load in a distributed network. A unique UPQC system is based on a three-level neutral position clamped inverter using intelligent control techniques.[2–5,16] A reduced rating star-connected transformer-based UPQC conditioner with the distributed generator for performance investigation for power quality improvement uses the technique of Simple Control Strategies of the Active Filters to reduce the harmonic distortion.[6,7,13,15]

This approach has the capability of voltage distortion mitigation as well as current harmonics compensation and there has been an increasing demand for DG. In recent years, to minimize the gap between the supply and load demand, which introduces some voltage and current disturbance and harmonics due to the generator types and the interfacing power electronics converters. UPQC has provided better current and voltage compensation with improved ripple attenuation capability while using reduced passive components. Moreover, an appropriate reduction in common DC link voltage is also achieved.[8–10,14] The control strategy aims to regulate the load voltage and the source current to the desired references in spite of the existence of harmonic components in the supply voltage and the load current, possible sag or swell in the supply voltage, and nonunity power factor of the supply side. Kalman filters are used to extract the fundamental as well as the harmonic components abovementioned, which will then be used to formulate the desired references and those regarded as measurable disturbances, respectively. A hybrid system mainly consists of a proton exchange membrane fuel cell and the fuel cell also

Int. J. Wavelets Multiresolut Inf. Process. Downloaded from www.worldscientific.com
by UNIVERSITY OF NEW ENGLAND on 01/01/20. Re-use and distribution is strictly not permitted, except for Open Access articles.

includes ultra capacitor-based UPQC. With the load sharing point, the UPQC system can handle a wide range of power quality issues and it can be compensated and the voltage quality will be improved in the distribution network.[11,17,21,24] High-performance UPQC uses command generator tracker-based direct adaptive control strategy.[19]

The Power Control strategies have been using a single stage converter for a grid-connected micro grid system to reduce the multiple DC-AC-DC conversions in an individual AC or DC grid. These micro grids with the proposed converters are applied to global renewable energy sources which will lead to maximum utilization of power at environmental free conditions with low losses improving the efficiency of the system neuro-fuzzy controller for frequency tracking and extraction of harmonics in grid voltage and load currents.[12,20,22] The performance of the proposed UPQC control scheme is significantly improved compared with the conventional control strategy owing to the superiority of the resonant controllers. Also, voltage sag/harmonic and current harmonic detectors are not required in the proposed control scheme, which help to simplify the control strategy and to improve the control accuracy of the devices that can simultaneously and independently control both the real and reactive power qualities in a transmission line.[23]

3. Materials and Method

The power quality issue can happen from multiple points of view in the distribution framework. Be that as it may, any of the reasonable compensators all around are fine to take care of the issues and enhance the power quality in distribution power framework. The grid-associated framework for building up the power quality at Point of Common Coupling (PCC) is displayed in Fig. 1. Mostly, it comprises a

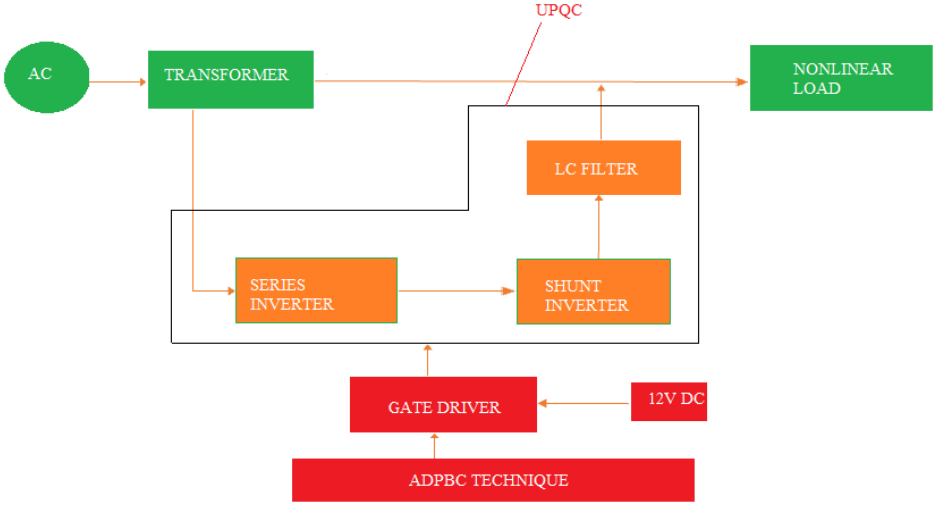


Fig. 1. Block diagram.

Int. J. Wavelets Multiresolut Inf. Process. Downloaded from www.worldscientific.com
by UNIVERSITY OF NEW ENGLAND on 01/01/20. Re-use and distribution is strictly not permitted, except for Open Access articles.

pay component, for example, UPQC, Shunt inverter, Series inverter, LC channel, adaptive distributed power balanced control (ADPBC) system and unbalanced load. The control arrangement of the pay plot infuses a symphonious free current into the grid framework. To enhance the power factor, the reactive piece of the load current and the harmonics in the enlistment generator current are counterbalanced by infusing the inverter output current of the compensating device, hence building up the power quality of the grid. To fulfill these, the grid voltages are synchronized while creating the current command for the inverter in the control arrangement of the compensating device.

The UPQC is a consolidation of both series filter and shunt active filter in a consecutive setup, which prevents voltage and current fluctuations and power factor correction in distribution supply. UPQC can remunerate current symphonious reactive power, voltage distortions and control load stream yet cannot counterbalance voltage interference due to not having sources. Consequently, in this work, proposed adaptive distributed power adjust control is helpful to UPQC framework as the releasing time of the DC connect capacitor is kept at a lower level. As per the needs, the framework execution is upgraded drastically.

The general structure of proposed ADPBC-based UPQC comprises two inverters, and it is associated with a predisposition voltage generator as appears in Fig. 1.

3.1. *Three phase UPQC*

In this work, the Four-leg Voltage source inverter (VSI) is considered to compensate the neutral current passing through the Transformer Neutral point. The fourth leg is added to the current three-phase three-wire (3P3W) UPQC, with the ultimate goal of the transformer neutral point being virtual zero possible. In this way, the proposed system will understand the three-phase four-wired (3P4W) framework from a 3P3W system at the end of the delivery load.

This would result in the long-run outcome in natural extension from 3P3W to 3P4W structure. To understand the standard reference source on condition of unbalanced load currents produced similarly, another control technique is proposed in this work. The UPQC has essentially three-phase series transformers to relate one of the inverters in the line–line and work as a limited voltage source. This system can perform from a 3P3W architecture without much of a stretch if a 3P4W system can use three-phase serial transformer neutral for a neutral wire interface to understand the 3P4W structure at that time. The three-phase four-wire UPQC schematic outline appears in Fig. 2.

The neutral current is displayed moving towards the fourth wire through the neutral point of the transformer. As a part of the neutral current, graph can be remunerated by applying shunt capacitor or inverter topology to the four-leg VSI topology. A four-legged VSI topology division requires an extra leg while contradicting the spilt capacitor topology. The neutral current play in the four-leg VSI architecture is essentially more than double the size of the capacitor.

Int. J. Wavelets Multiresolut Inf. Process. Downloaded from www.worldscientific.com
by UNIVERSITY OF NEW ENGLAND on 01/01/20. Re-use and distribution is strictly not permitted, except for Open Access articles.

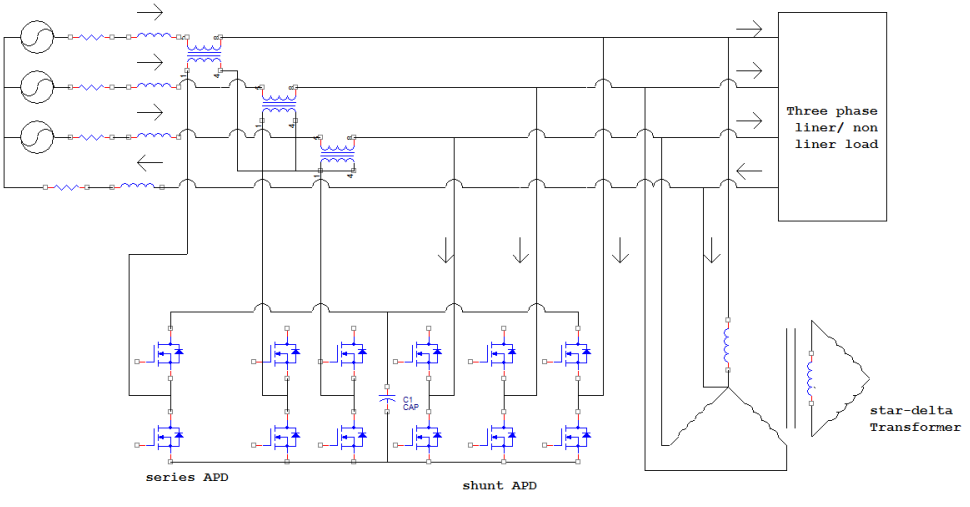


Fig. 2. Three phase four wire UPQC schematic diagram.

Bring about more complex control loop to keep the dc bus voltage at a steady level.

3.1.1. *ADPBC control algorithm for* 3*P*4*W UPQC system*

The control method for continuous series active filter (APF) depends on the generation conspiracy of the unit vector system, while the APF's control system is discussed in this section. In the light load condition 3P4W system, the current drawn from the distribution is in unbalanced condition. In this work, another control method is introduced with the current imbalance display on load current through the concept of a single-phase p–q hypothesis. A multi-stage structure can be categorized as a simulated two-stage structure by providing a rib/2 lead or $\pi/2$ slack indicated by this description, that is, the current three autonomous two-dimensional boundaries of the voltage and the first three-phase form at each stage. The resulting two-phase structures α–β spoken directions and, accordingly, the balance of the three-phase unbalanced framework structure is connected to the p–q hypothesis used in each case. Actual load voltages and load currents are considered as α-pivot levels, while the $\pi/2$ Front Load or $\pi/2$ Slack voltages and $\pi/2$ lead or $\pi/2$ Slack load currents are considered β-axis measurements. In this work, the $\pi/2$ lead is considered to fulfill each step-by-step two-phase system. A significant disadvantage of the p–q hypothesis gives the worst effects under the distorted and random input/application voltages. Measured load voltage signals, separated for the continuous APF in understanding the ultimate goal of removing these limitation, are used more than actual load voltages.

Int. J. Wavelets Multiresolut Inf. Process. Downloaded from www.worldscientific.com
by UNIVERSITY OF NEW ENGLAND on 01/01/20. Re-use and distribution is strictly not permitted, except for Open Access articles.

For phase a, the load voltage and current in α–β coordinates can be represented by $\pi/2$ lead as

$$\begin{bmatrix} V_{L\alpha-\alpha} \\ \mathrm{V}_{L\alpha-\beta} \end{bmatrix} = \begin{bmatrix} V^*_{L\alpha}(wt) \\ V^*_{L\alpha}\left(wt + \dfrac{\pi}{2}\right) \end{bmatrix} = \begin{bmatrix} V_{Lm}\sin(wt) \\ V_{Lm}\cos(wt) \end{bmatrix}, \tag{1}$$

$$\begin{bmatrix} i_{L\alpha-\alpha} \\ i_{L\alpha-\beta} \end{bmatrix} = \begin{bmatrix} i_{L\alpha}(wt + \varphi L) \\ i_{L\alpha}(wt + \varphi L) + \dfrac{\pi}{2} \end{bmatrix}, \tag{2}$$

where $V_{L\alpha}(wt)$ is the load voltage, V_{Lm} is the desired load voltage magnitude.

The load voltage and current of A–β coordination are represented by the leading $p\pi/2$ lead as

$$\begin{bmatrix} V_{Lb-\alpha} \\ V_{Lb-\beta} \end{bmatrix} = \begin{bmatrix} V^*_{Lb}(wt) \\ V^*_{Lb}\left(wt + \dfrac{\pi}{2}\right) \end{bmatrix} = \begin{bmatrix} V_{Lm}\sin(wt - 120^\circ) \\ V_{Lm}\cos\left(wt - 120^\circ\right) \end{bmatrix}, \tag{3}$$

$$\begin{bmatrix} i_{Lb-\alpha} \\ i_{Lb-\beta} \end{bmatrix} = \begin{bmatrix} i_{Lb}(wt + \varphi L) \\ i_{Lb}(wt + \varphi L) + \dfrac{\pi}{2} \end{bmatrix}. \tag{4}$$

In adding, for phase c, the load voltage and current

$$\begin{bmatrix} V_{Lc-\alpha} \\ V_{Lc-\beta} \end{bmatrix} = \begin{bmatrix} V^*_{Lc}(wt) \\ V^*_{Lc}\left(wt + \dfrac{\pi}{2}\right) \end{bmatrix} = \begin{bmatrix} V_{Lm}\sin(wt + 120^\circ) \\ V_{Lm}\cos(wt + 120^\circ) \end{bmatrix}, \tag{5}$$

$$\begin{bmatrix} i_{Lc-\alpha} \\ i_{Lc-\beta} \end{bmatrix} = \begin{bmatrix} i_{Lc}(wt + \varphi L) \\ i_{Lc}(wt + \varphi L) + \dfrac{\pi}{2} \end{bmatrix}. \tag{6}$$

By utilizing the meaning of balanced three-phase framework for hypothesis of p–q, the prompt active instantaneous power is to be considered.

$$P_{L,abc} = \nu_{L,abc-\alpha}.i_{L,abc-\alpha} + \nu_{L,abc-\beta}.i_{L,abc-\beta\alpha}. \tag{7}$$

Instantaneous reactive power

$$q_{L,abc} = \nu_{L,abc-\alpha}.i_{L,abc-\beta} + \nu_{L,abc-\alpha}. \tag{8}$$

The phase-α can be viewed immediately by the load and the reactive powers are denoted as given below

$$\begin{bmatrix} P_{La} \\ q_{La} \end{bmatrix} = \begin{bmatrix} V_{La-\alpha} & V_{La-\beta} \\ -V_{La-\beta} & V_{La-\alpha} \end{bmatrix} \cdot \begin{bmatrix} i_{La-\alpha} \\ i_{La-\beta} \end{bmatrix}, \tag{9}$$

where

$$P_{La} = \bar{P}_{La} + \tilde{P}_{La}, \tag{10}$$

$$q_{La} = \bar{q}_{La} + \tilde{q}_{La}. \tag{11}$$

In (10) and (11), P_{La} and q_{La} speak to the DC parts that are in charge of important load active and reactive powers, while $\tilde{P}_{La}$ and $\tilde{q}_{La}$ talk to the AC segments that

Int. J. Wavelets Multiresolut Inf. Process. Downloaded from www.worldscientific.com
by UNIVERSITY OF NEW ENGLAND on 01/01/20. Re-use and distribution is strictly not permitted, except for Open Access articles.

are in charge of harmonics powers. A low-pass filter using first immediate phase-by-load, active and reactive power components can be removed from P_{La} and q_{La} separately. Therefore, the active power is provided by the central load immediately for phase one.

$$P_{La}, 1 = \bar{P}_{La}. \tag{12}$$

An instant basic load reaction power given to the grid given by

$$q_{La}, 1 = \bar{q}_{La}. \tag{13}$$

Likewise, the central instantaneous load active and reactive load powers for the fundamental instantaneous phases and c active power load can be shown as critical for instantaneous phase b

$$P_{Lb}, 1 = \bar{P}_{Lb}. \tag{14}$$

The instantessential load reactive power for phase b is given by

$$q_{Lb}, 1 = \bar{q}_{Lb}. \tag{15}$$

Instantaneous fundamental load active power for phase c

$$P_{Lc}, 1 = \bar{P}_{Lc}. \tag{16}$$

The instantaneous fundamental load reactive power for phase c is given by

$$q_{Lc}, 1 = \bar{q}_{Lc}. \tag{17}$$

Since each load current is drawn for each phase because the number of available loads accordingly, for every system in the primary load is active power and reactive power of immediate interest the load may not be identical.

So, this load is the linear and balanced load of the total load viewed by the application to be redistributed between the applications, UPQC, and load that ultimately is the objective of the unbalanced load power, as a consummately consistent three-phase shunt active filter found in the application view is the method of unbalanced load. The unbalanced or balanced reactive power demanded by the load shunt APF should be taken care of by shunt active power filter.

The previously mentioned undertaking essential load instantaneous active power can be accomplished by summing all the three phases of request of every utility phase and redistributing it again

$$P_{L,\text{total}} = P_{La}, 1 + P_{Lb}, 1 + P_{Lc}, 1, \tag{18}$$

$$P^*_{s/ph} = \frac{P_{L,\text{total}}}{3}. \tag{19}$$

Condition (19) gives the crucial active redistributed per-phase power supply should request that each phase utility keeps the end goal in mind to accomplish perfectly balanced source currents. From (19), it is evident that under each of the conditions, the total power is derivative from the utility but with the perfectly balanced way

Int. J. Wavelets Multiresolut Inf. Process. Downloaded from www.worldscientific.com
by UNIVERSITY OF NEW ENGLAND on 01/01/20. Re-use and distribution is strictly not permitted, except for Open Access articles.

despite the fact that load currents are unbalanced. Therefore, the reference recompensing currents to form accurate balanced three-phase system can be removed by taking the reverse of (9)

$$\begin{bmatrix} i^*_{sa-\alpha} \\ i^*_{sa-\beta} \end{bmatrix} = \begin{bmatrix} V_{La-\alpha} & V_{La-\beta} \\ -V_{La-\beta} & V_{La-\alpha} \end{bmatrix} . \begin{bmatrix} p^*_{s/ph} + P_{dc/ph} \\ 0 \end{bmatrix}. \tag{20}$$

In, P (dc/ph) is the exact measure of per-phase active power taken from the source that should to be to keep up the DC-voltage at a consistent level and to interface with related UPQC system. The wavering instantaneous active power P should be traded between the load and shunt APF. The reactive power term (V_{La}) in (20) is measured as zero since the utility should not provide load reactive power request. In the above system, *a-pivot* reference current communicates to the dominant source current, since a-axis amounts have a place with the first framework under thought and the β-axis reference repaying current/2 lead concerning the first structure.

Therefore,

$$t^*_{sa}(t) = \frac{V_{La-\alpha(t)}}{V^2_{La-\alpha} + V^2_{La-\beta}} . [p^*_{\frac{s}{ph}} + p_{dc/ph}(t)]. \tag{21}$$

Similarly, phase B and C are the estimated current reference source,

$$i^*_{sb}(t) = \frac{V_{Lb-\alpha}(t)}{V^2_{Lb-\alpha} + V^2_{Lb-\beta}} . [p^*_{\frac{L}{\text{ph}}}(t) + p_{dc/ph}(t)], \tag{22}$$

$$i^*_{sc}(t) = \frac{V_{Lb-\alpha}(t)}{V^2_{Lb-\alpha} + V^2_{Lb-\beta}} . [p^*_{\frac{L}{\text{ph}}}(t) + p_{dc/ph}(t)], \tag{23}$$

The reference neutral current source can be extracted by simply adding all the sensed load currents without actual neutral current sensing as

$$i_{Ln}(t) = i_{La}(t) + i_{Lb}(t) + i_{Lc}(t), \tag{24}$$

$$i^*_{sh-n(4)} = i_{L-n(t)}. \tag{25}$$

The Basic Active Power Validation PI Regulator is based on the proposed DC Connection Voltage Control Loop, the current generation of the reference source is given as follows Eqs. (21)–(23).

3.2. *Single-phase UPQC*

Figure 3 shows the power circuit of proposed UPQC. It contains two DC side capacitors in a single phase structure. The center point of the capacitors C1 and C2 is related with and has utility considered as neutral point of the reference voltages in the inverter circuit. The two arms of inverter might work separately. The combination of transistors Q1 and Q2 is used for improving the voltage using segregation transformer TR, coupling inductance L_d and filter capacitance Cd for counteracting the varied voltage harmonics, voltage hang and swell. For accurate power stabilization, the power circuit is proportional to SAF UPQC system. The voltage across

Int. J. Wavelets Multiresolut Inf. Process. Downloaded from www.worldscientific.com
by UNIVERSITY OF NEW ENGLAND on 01/01/20. Re-use and distribution is strictly not permitted, except for Open Access articles.

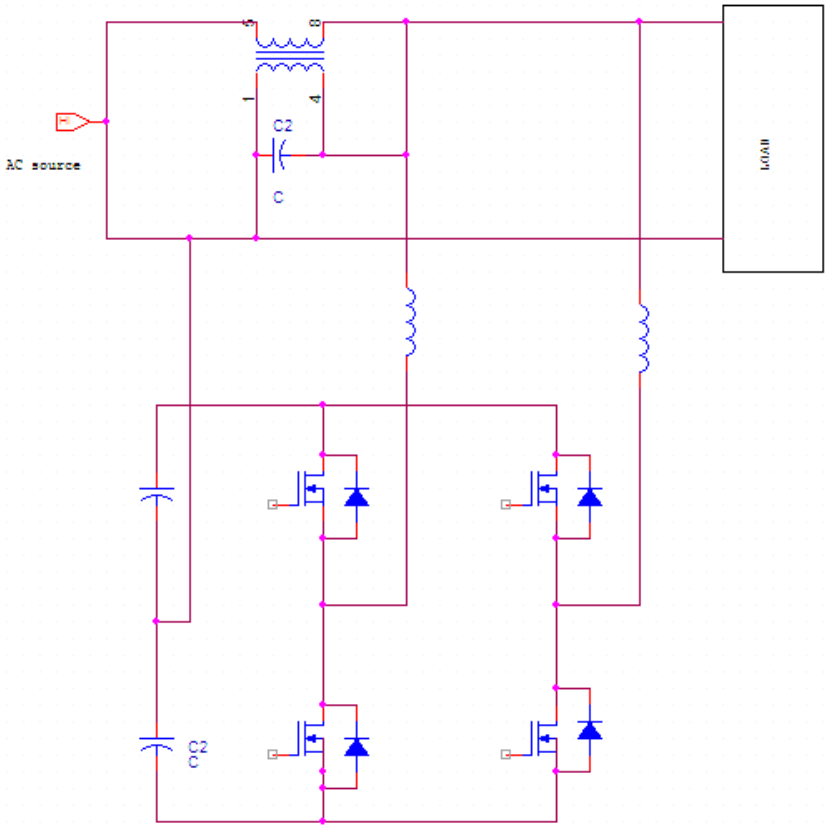


Fig. 3. Circuit diagram for the UPQC system.

the capacitor Cd compensation reference voltage should follow. Using L_d makes it possible to get a smooth voltage variation through. The Cd is large enough to have a constant voltage output capacitor during each switching interval so the current of inductor L_d varies smoothly and is almost linear in form.

The pair of the transistors Q3 and Q4 of PAF go about and adjusts for regular UPQC current harmonics and reactive power of the nonlinear load. Utilizing coupling inductor, the capacitors C1 and C2 charge to La makes it conceivable like a boost converter, and it moreover smoothens the compensation current $i\text{comp}_{(t)}$. Figure 4 demonstrates a common power circuit system for single-phase UPQC. It comprises two H-bridge connected inverters. One of the works as a general series inverters for active filter adjusts the voltage supply and voltage quality, and the following one works as a nonlinear shunt active filter for harmonics and reactive power load. Comparison of Figs. 3 and 4 show that the number of switches is half of the power circuit of Figs. 3 and 4. Also, the split on the DC side capacitors in Fig. 3 provide a neutral point which might be used as the control circuit for zero potential.

Int. J. Wavelets Multiresolut Inf. Process. Downloaded from www.worldscientific.com
by UNIVERSITY OF NEW ENGLAND on 01/01/20. Re-use and distribution is strictly not permitted, except for Open Access articles.

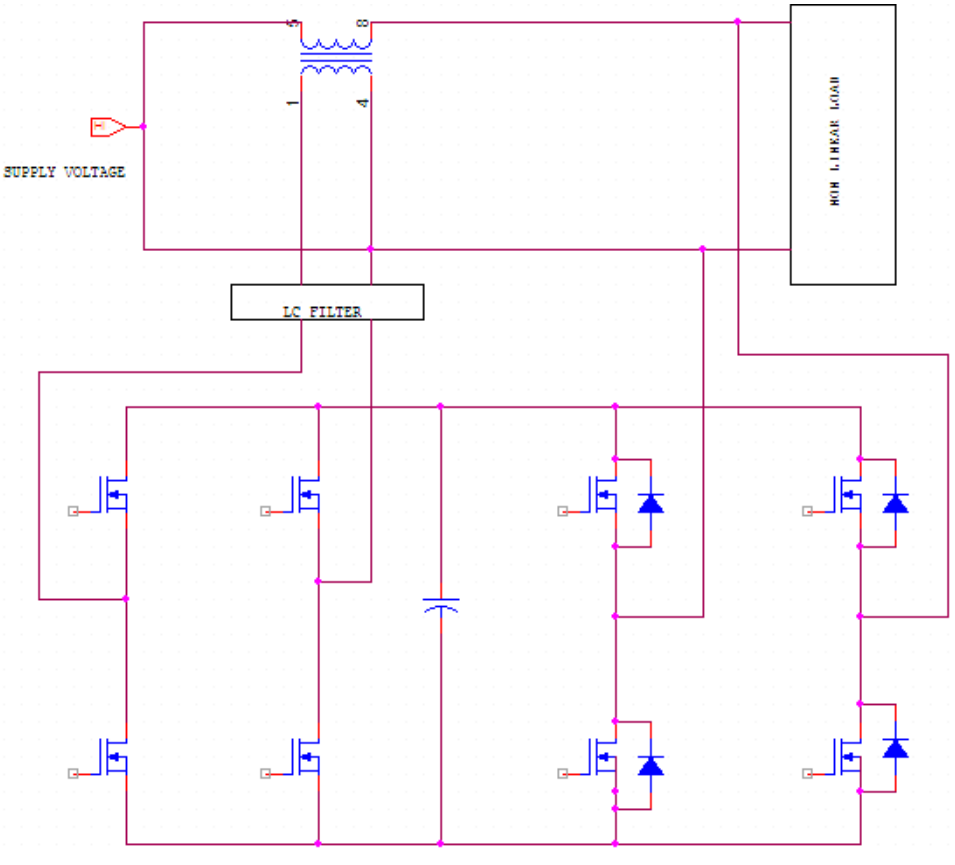


Fig. 4. General power circuit topology of single-phase UPQC.

3.2.1. *Control strategies of shunt active filter*

The shunt APF works as a controllable current source to evacuate the harmonic input current. The consonant parts of the single-phase nonlinear load current Li are made out of the odd terms, i.e. $(2n+1)\text{th}(n=1,2,3\ldots)$

$$i_L = i_{L1} + i_{Ln} = I_{L1}\sin(wt-\theta_{L1}) + \sum_{n=3,5,7} \ldots I_{LK}\sin(hWt-\theta_{Ln}). \qquad (26)$$

In this work, the supply current i_s is accurately measured and controlled to be sinusoidal. The d and q segments of the supply current i_s in $dq0$ outline is shown in the following condition:

$$\begin{bmatrix} i_{sd} \\ i_{sq} \end{bmatrix} = \begin{bmatrix} \cos\theta & \sin\theta \\ -\sin\theta & \cos\theta \end{bmatrix} \begin{bmatrix} i_{s\alpha} \\ i_{s\beta} \end{bmatrix}. \qquad (27)$$

The supply current i_s segments in $dq0$ outline are made out of the DC segment and the even harmonics. Keeping in mind the end goal to manage the supply current

Int. J. Wavelets Multiresolut Inf. Process. Downloaded from www.worldscientific.com
by UNIVERSITY OF NEW ENGLAND on 01/01/20. Re-use and distribution is strictly not permitted, except for Open Access articles.

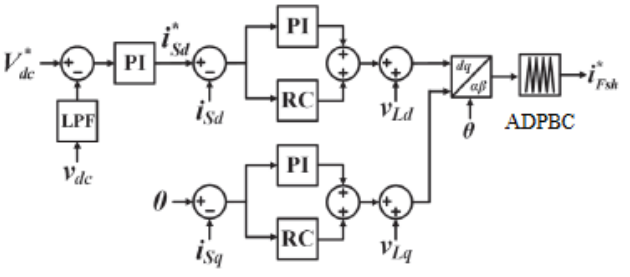


Fig. 5. Block diagram of RC.

in $dq0$ outline, the PI and the altered RC controller are utilized: PI controller directs the central part of the supply current which is the DC segment in original $dq0$ outline, in the interim, a charged RC controls in the AC harmonic segments. The primary normal for the RC is comparable to an arrangement of the resounding controllers, which can all the while track a substantial number of harmonic currents or voltages.

The block diagram of the RC is shown in Fig. 5 and the transfer functions of the PI controller and the RC in the continuous time domain are given in the following equations, respectively:

$$G_{p1}(s) = K_p + \frac{K_i}{s}, \tag{28}$$

$$G_{\mathrm{RC}}(s) = \frac{K_T Q(s) e^{-} STd}{1 - Q(s) e^{-} STd}, \tag{29}$$

where K_P is the proportional gain, K_i is the integral gain, T_d is the time delay of the RC, Q is the filter transfer function and K is the RC gain. When the time delay term Td in (29) is selected to be the same value as the fundamental period Tp of the supply voltage, it has a slow dynamic response because of the long time delay. To overcome this problem, the delay time is reduced to half of the fundamental frequency $T_d = \frac{T_p}{2}$ because the even harmonic components exist in $dq0$ frame as given in (30). In case of $(T_d = \frac{T_p}{2})$, the transfer function of the RC for the single-phase UPQC can be rewritten as follows:

$$G_{\mathrm{Rc}}(S) = \frac{K_r Q(s) e^{-STp/2}}{1 - Q(s) e^{-STp/2}}. \tag{30}$$

3.2.2. *Control strategy for series APF*

The series APF remunerates the contorted source V_s to keep up the load voltage V_L sinusoidal. The distorted supply voltage is made out of the central part V_{s1} and harmonics S_{hv}

$$V_s = V_{s1} + V_{sh} = V_{s1} \sin(wt) + \sum_{h=3,5,7} V_{sh} \sin(hwt - \theta_{sh}). \tag{31}$$

Int. J. Wavelets Multiresolut Inf. Process. Downloaded from www.worldscientific.com
by UNIVERSITY OF NEW ENGLAND on 01/01/20. Re-use and distribution is strictly not permitted, except for Open Access articles.

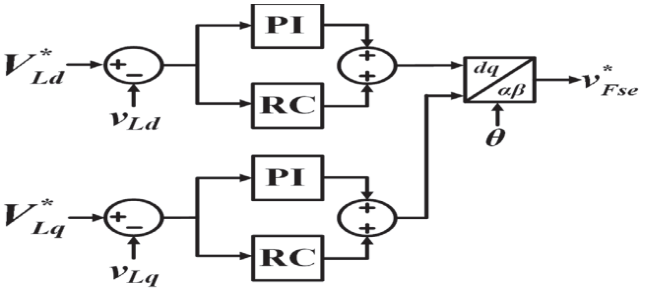


Fig. 6. Harmonic detector.

Like the control plan of the shunt APF, the reference voltage for the series APF V_{fse} is created without the voltage list identifier or the harmonic indicator as portrayed in Fig. 6.

In addition, it has just a single voltage control loop. Hypothetically, the desired load voltage in $dq0$ frame can be characterized as follows:

$$V_{Ld}^{*} = V_{L1}^{*}, \tag{32}$$

$$V_{Lq}^{*} = 0. \tag{33}$$

3.3. *Mathematical model of ADPBC for power quality improvement*

The power quality issue is a nonlinear optimization issue. The level of nonlinearity causes challenges in taking care of this problem utilizing traditional techniques. Subsequently, one of the exact stochastic pursuit methods called ADPBC has been connected to take care of the power quality issue in this work. ADPBC is a decline-based stochastic inquiry strategy that starts with an underlying populace of frogs whose qualities, known as images, speak to the choice factors. In this algorithm, singular frogs are not very renowned; instead, they are viewed as hosts for images and depicted as a memetic vector. The algorithm incorporates components of neighborhood seek and global data switching.

In ADPBC, the total populace is divided into gatherings (image lexes) that hunt autonomously. Partition is done as takes after: the populace is separated into q image lexes which each contain p frogs. In this way, the primary frog goes to the main memeplex, the second frog continues to the next memeplex, frog p goes to the qth memeplex, and frog $p + 1$ backpedals to the ultimate memeplex, and so on. In each memeplex, the frogs with the best and the most noticeably bad finesse are recognized as Xb and Xw, separately. Likewise, the frog with the most prepared wellness level among all the image lexes is named Xg. At that point, the accompanying procedure is connected to enhance just the frog with the most exceedingly terrible wellness in each cycle. Like this, the position of the frog with

Int. J. Wavelets Multiresolut Inf. Process. Downloaded from www.worldscientific.com
by UNIVERSITY OF NEW ENGLAND on 01/01/20. Re-use and distribution is strictly not permitted, except for Open Access articles.

the most exceedingly awful welfare is balanced as takes after:

$$C_i = \text{rand}(0).(Xb - Xw), \tag{34}$$

$$Xw(\text{new}) = Xw + C_i, \tag{35}$$

$$-C_{\max} \leq C_i \leq C_{\max}, \tag{36}$$

where rand(0) is the random number between 0 and 1 and C max is the maximum allowed for a change in a frog's position.

On the off chance that this procedure gives a preferred arrangement, it replaces the most noticeably awful frog in each memeplex, another methodology to help the disadvantaged. This new mode called ADPBC will be displayed in subtle elements in the accompanying segment. The objective of the general procedure is to decide ideal worldwide arrangements. Be that as it may, it is troublesome for ADPBC algorithm to beat neighborhood minima when dealing with some entangled capacities. Along these lines in this work, an ADPBC is proposed to overcome this weak point. In such manner, all the best arrangements in each memeplex (Xb) and the arrangement with the most qualified wellness level among all the image lexes (Xg) are characterized, at that point, the accompanying procedure is connected to produce mutation vector. It is necessary to note that the mutation vector dimension is equal to the meme lexes number.

$$X^i_{\text{mul}} = X^{\text{rand}}_{\text{mul}} + \text{rand}(0)(X^i_b - X^i_{\text{rand}}) + \text{rand}(.)(X^i_g - X^i_{\text{rand}}), \quad i = 1, 2, \ldots, N\text{mem}, \tag{37}$$

where Xb is the best result in each memeplex, Xg is the best solution in all memeplexes, i Xrand is a randomly generated vector, rand () is a random number between 0 and 1 and Nmem is the number of memeplexes. If the generation cost of the trial vector X^i_{mul} is better than that of the target vector, i.e. X^i_g, the target vector is replaced with the trial vector in the next generation. In this way, converging of the global optima can be guaranteed and also getting stuck in a local optimum solution can be prevented.

3.4. *Apply ADPBC for power quality problems*

The application of ADPBC on the power quality problem with custom power distribution devices is presented. To apply the ADPBC algorithm to solve this problem, the following steps should be taken and repeated.

Figure 7 demonstrates the flow diagram of ADPBC controlling strategy. The crucial blunder was decided by adding the error to a gatherer, and the subordinate blunder was computed by subtracting the mistake from the past oversight. Each time the control circle executes, each of these steps is consistent to increase that has been tuned to improve reaction time and exactness. These mistakes, duplicated by their gain constants are then increased by the value of figure in the new control esteem. Along these lines, the control parameter is continuously refreshed in light of the reaction of the UPQC.

Int. J. Wavelets Multiresolut Inf. Process. Downloaded from www.worldscientific.com
by UNIVERSITY OF NEW ENGLAND on 01/01/20. Re-use and distribution is strictly not permitted, except for Open Access articles.

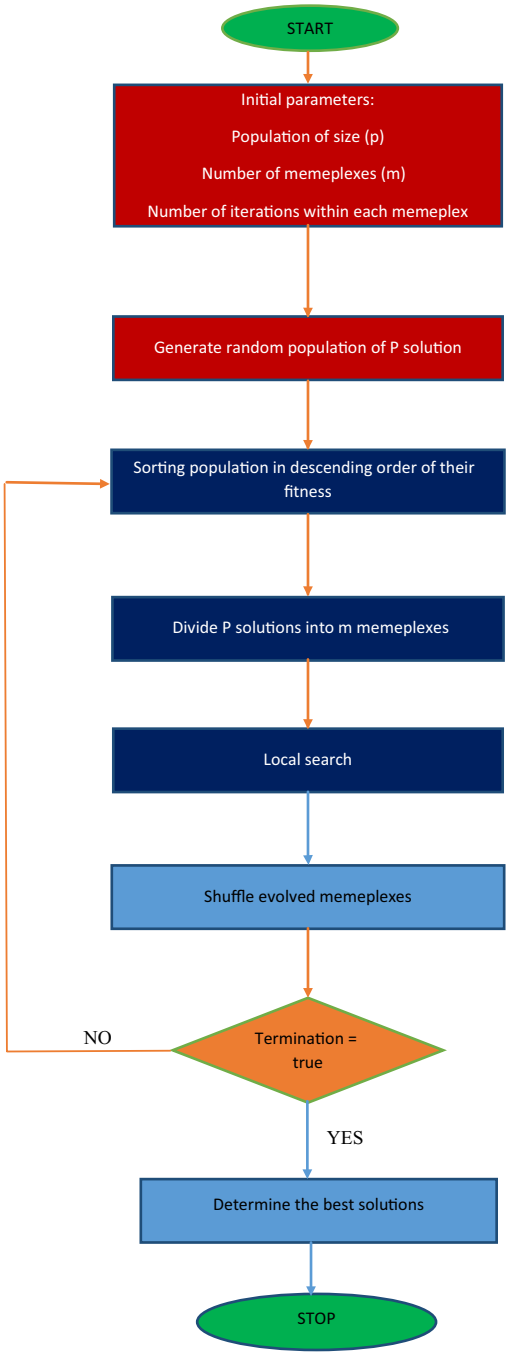


Fig. 7. Flow chart for ADPBC.

Int. J. Wavelets Multiresolut Inf. Process. Downloaded from www.worldscientific.com
by UNIVERSITY OF NEW ENGLAND on 01/01/20. Re-use and distribution is strictly not permitted, except for Open Access articles.

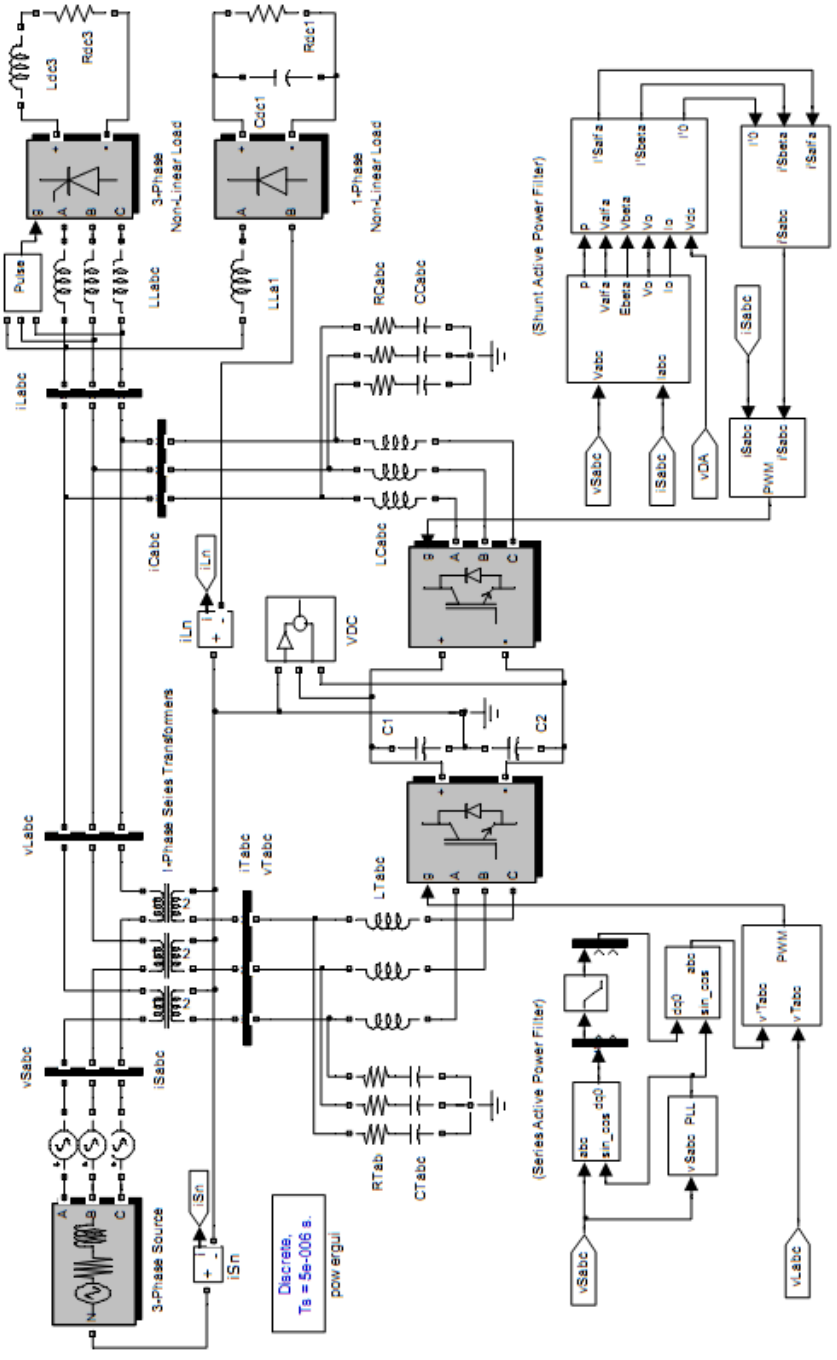


Fig. 8. Three-phase four-wire UPQC.

Int. J. Wavelets Multiresolut Inf. Process. Downloaded from www.worldscientific.com
by UNIVERSITY OF NEW ENGLAND on 01/01/20. Re-use and distribution is strictly not permitted, except for Open Access articles.

Algorithm.

Step 1: Create the initial population. The initial population for each iterate is random. Created as takes after:

$$\text{population} = \begin{bmatrix} X1 \\ X2 \\ \cdots \\ Xf \end{bmatrix}$$

$$Xi = [\text{Vstack}, \text{Vpv}, \text{Ppv}, \text{CUSTOM}_{\text{parameters}}, Qc]$$

where Vstack and VPV are voltages of the slack transport and PV transports separately, PPV is active power generation of PV transports, $\text{CUSTOM}_{\text{parameters}}$ include points of shunt converter, series converter and amplitude of series converter and QC is reactive power estimation of the compensator capacitor.

Step 2: Compute target work an incentive for each.

Step 3: Sort the initial population in light of the target work estimates with diminishing way.

Step 4: Isolating arranged population in memeplexes by the accompanying procedure, the main population goes to the principal memeplex, the second population proceeds to the second memeplex, population qth goes to the qth memeplex, and population $q+1$ moves in reverse to the starting memeplex, and so on.

Step 5: Select the best and most exceedingly bad population in each memeplex and generate the $_b$s and X_w for them separately.

Step 6: The frog with the global best wellness in all memeplexes is recognized as Xg.

Step 7: A procedure is connected to enhance just the frog with the most exceedingly awful wellness, as per this, the procedure delivers a superior arrangement; it replaces the most exceedingly awful frog. Something else, another population, is randomly created to supplant that population. This procedure proceeds for a particular number of cycles (itetationmax1).

Step 8: In this segment, all memeplexes are joined and arranged once more.

Step 9: Apply change to repay ADPBC downsides specified in the past segment.

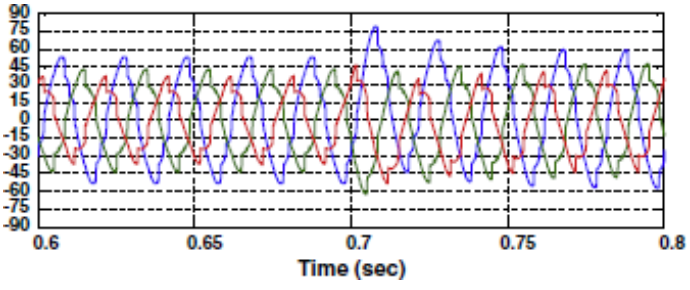
Step 10: In the event that the present cycle number (iterationmax2) achieves the foreordained most extreme emphasis number, the inquiry strategy is halted. Else, it goes to Step 4.

Step 11: The last Xg is the answer for the issue.

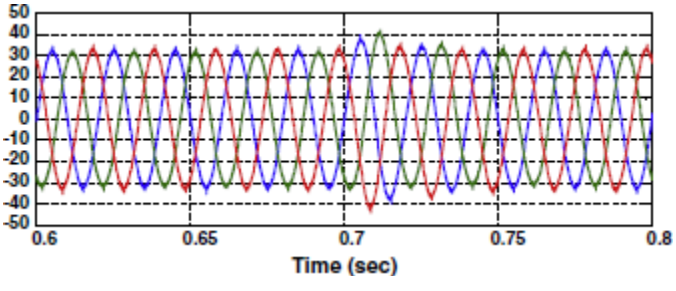
4. Results and Discussion

The simulation model for single-phase UPQC and three-phase UPQC control using ADPBC method has been successfully modeled and tested using MATLAB/SIMULINK toolbox. The performance in steady state condition is evaluated

Int. J. Wavelets Multiresolut Inf. Process. Downloaded from www.worldscientific.com
by UNIVERSITY OF NEW ENGLAND on 01/01/20. Re-use and distribution is strictly not permitted, except for Open Access articles.

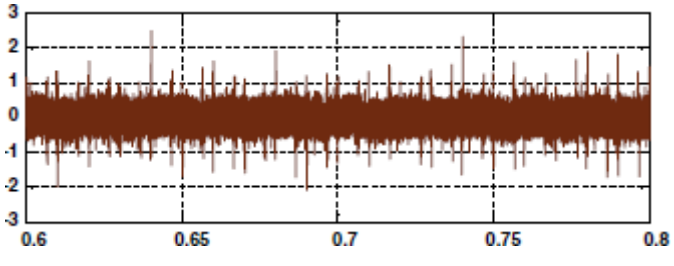


(a)

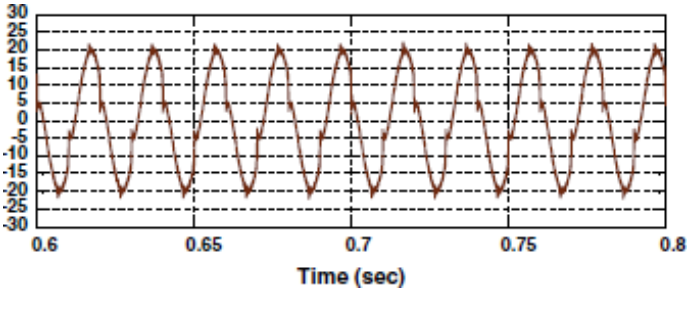


(b)

Fig. 9. (a) Three-phase unbalanced load current. (b) Three-phase balanced source current.



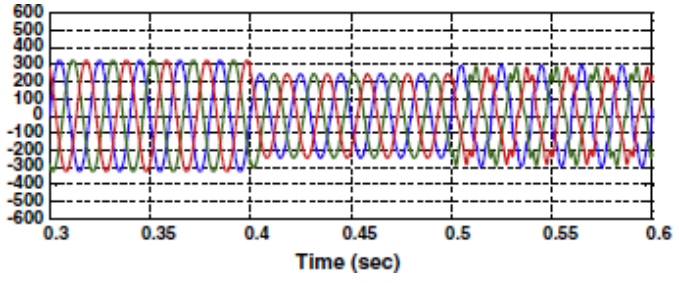
(a)



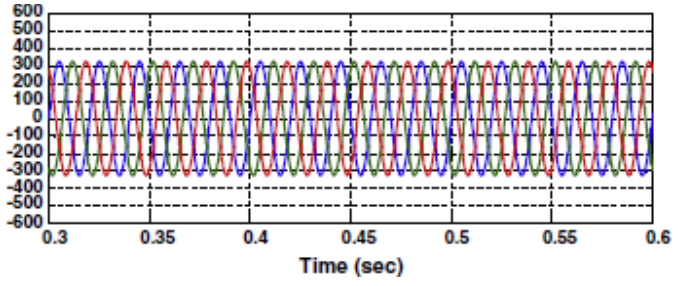
(b)

Fig. 10. (a) Source neutral current. (b) Compensating neutral current.

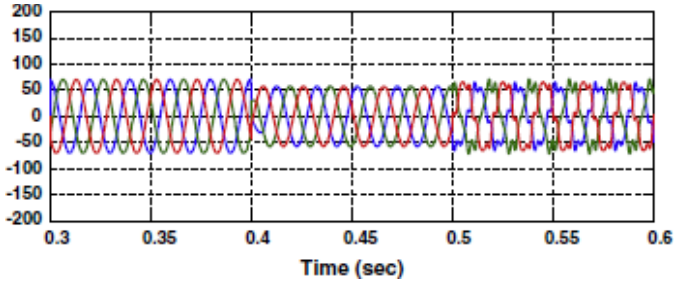
Int. J. Wavelets Multiresolut Inf. Process. Downloaded from www.worldscientific.com
by UNIVERSITY OF NEW ENGLAND on 01/01/20. Re-use and distribution is strictly not permitted, except for Open Access articles.



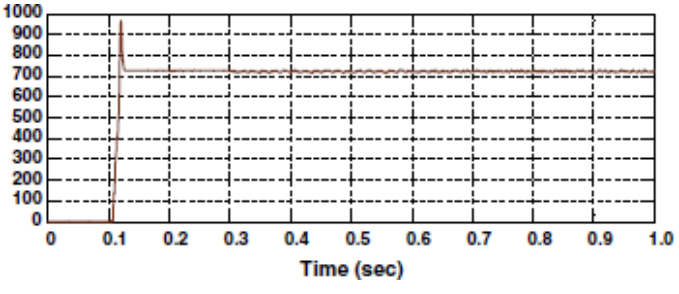
(a)



(b)



(c)



(d)

Fig. 11. (a) Three-phase source voltage. (b) Three-phase load voltage. (c) Three phase series injected voltage. (d) DC link capacitor voltage.

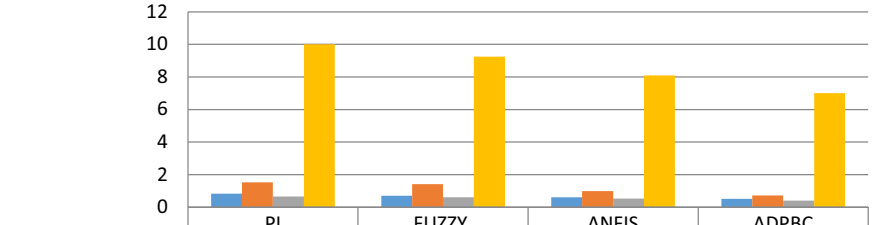
Int. J. Wavelets Multiresolut Inf. Process. Downloaded from www.worldscientific.com
by UNIVERSITY OF NEW ENGLAND on 01/01/20. Re-use and distribution is strictly not permitted, except for Open Access articles.

using different parameters. The proposed three-phase UPQC block diagram in Matlab/Simulink simulation software is shown in Fig. 8. The combination of series APF and shunt APF is connected to a common DC-link.

The three-phase diode bridge rectifier with a balance of plant load and the load is a combination of R-L, which acts as a load to create harmony.

Figures 9(a) and 9(b) show the three-phase balanced and unbalanced load and source current of the proposed adaptive distributed power balance control technique, as compared to other conventional techniques the proposed system provides better results.

Figures 10(a) and 10(b) show the source neutral current and compensating neutral current of the proposed adaptive distributed power balance control technique, as compared to other conventional techniques the proposed system provides better results.



	PI	FUZZY	ANFIS	ADPBC
execution time	0.8317	0.711	0.6102	0.512
steady state error	1.5325	1.4251	0.9914	0.73
switching loss	0.668	0.61	0.54	0.41
THD(%)	10	9.25	8.1	7.01

Fig. 12. Performance comparison of UPQC.

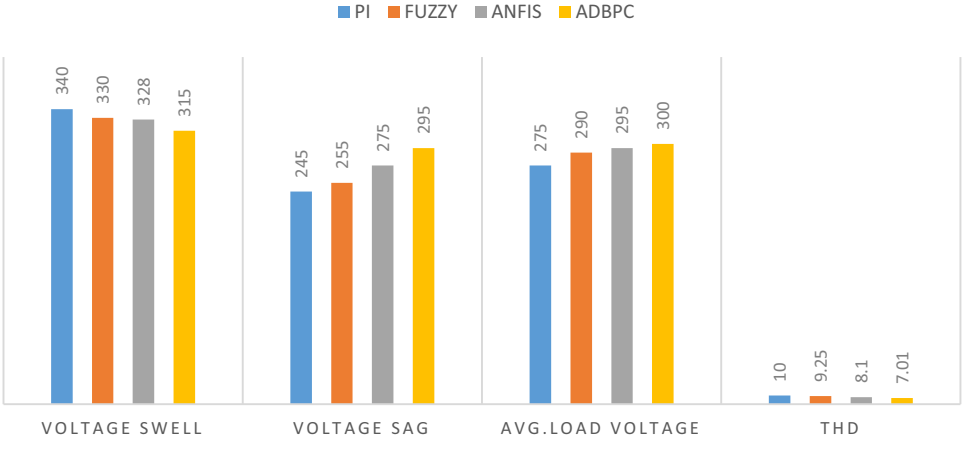


Fig. 13. Performance comparison for power quality improvement in different algorithms.

Int. J. Wavelets Multiresolut Inf. Process. Downloaded from www.worldscientific.com
by UNIVERSITY OF NEW ENGLAND on 01/01/20. Re-use and distribution is strictly not permitted, except for Open Access articles.

Figures 11(a) and 11(b) show the three-phase source voltage and load voltage of the proposed system. Figures 11(c) and 11(d) demonstrate the three-phase series injected voltage and DC capacitor link voltage of the proposed system. As compared to other conventional techniques the proposed system provides better results.

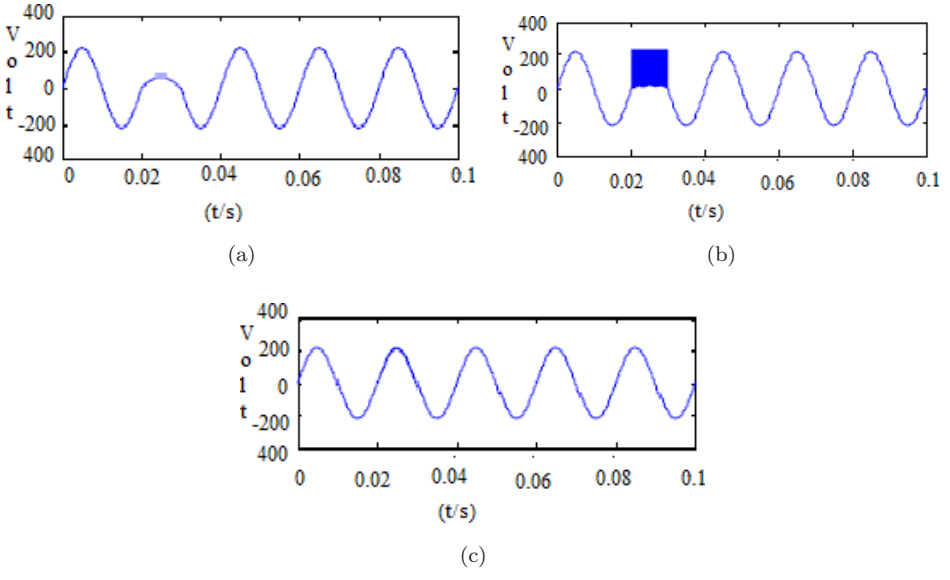


Fig. 14. Sag response of proposed system. (a) Sag waveform of grid voltage. (b) Output voltage before ADPBC. (c) Output voltage after ADPBC.

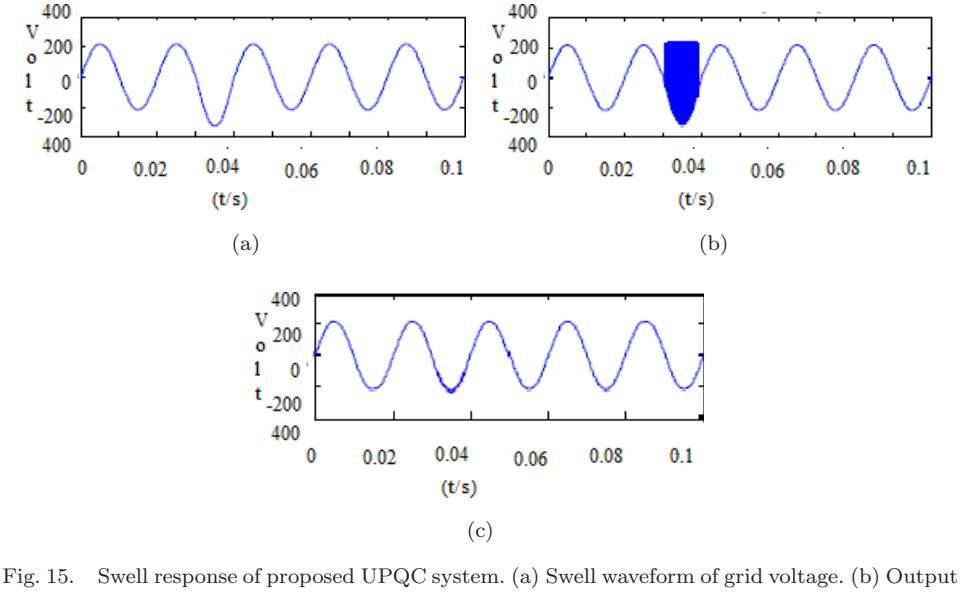


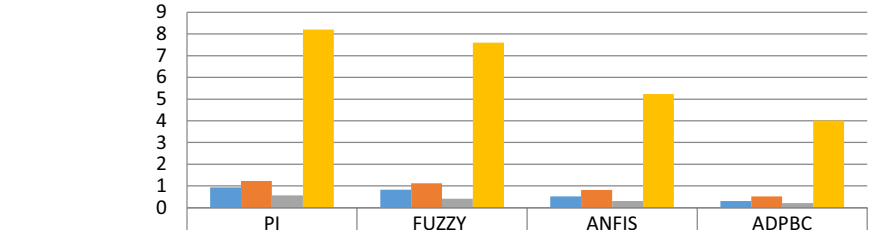
Fig. 15. Swell response of proposed UPQC system. (a) Swell waveform of grid voltage. (b) Output voltage before ADPBC. (c) Output voltage after ADPBC.

Int. J. Wavelets Multiresolut Inf. Process. Downloaded from www.worldscientific.com
by UNIVERSITY OF NEW ENGLAND on 01/01/20. Re-use and distribution is strictly not permitted, except for Open Access articles.

Figure 12 shows comparison of the UPQC controller action with various parameters such as execution time, steady state error, switching loss, and Total Harmonic Distortion (THD). From the simulation results, the comparison was mentioned in Fig. 12. The results prove that ADPBC-based controller provides better response overshoot than a conventional controller like PI, FUZZY and ANFIS.

Figure 13 shows the performance of various devices for the power quality improvement. The analysis clearly shows that the performance of the ADPBC method is comparatively better than the other conventional methods in terms of improving the power quality to its nominal values and reduction in harmonic levels.

Figure shows the single-phase UPQC voltage sag response of the proposed system. Figure 14(a) shows sag result of grid voltage, Fig. 14(b) shows the output response before applying the ADPBC in UPQC and Fig. 14(c) demonstrates the output voltage of UPQC after ADPBC technique is applied.



	PI	FUZZY	ANFIS	ADPBC
execution time	0.9317	0.825	0.517	0.301
steady state error	1.2325	1.1251	0.815	0.523
switching loss	0.564	0.41	0.31	0.21
THD(%)	8.2	7.6	5.23	4.01

Fig. 16. Performance comparison of UPQC.

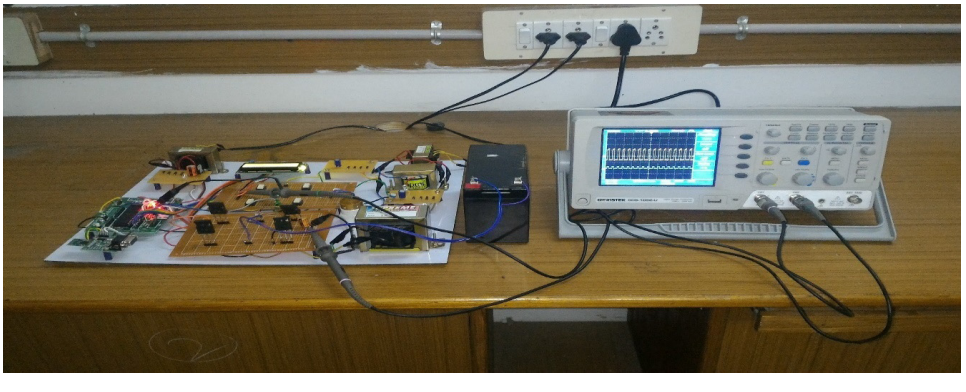


Fig. 17. Hardware setup.

Int. J. Wavelets Multiresolut Inf. Process. Downloaded from www.worldscientific.com
by UNIVERSITY OF NEW ENGLAND on 01/01/20. Re-use and distribution is strictly not permitted, except for Open Access articles.

Table 1. Comparison of features from different algorithm.

Compared features	PI	FUZZY	ANFIS	PROPOSED ADPBC
Cost	High	High	Medium	Low
Physical structure	Big	Big	Small	Small
Resistance to work environment	High	High	Medium	Low
Finding fault	Difficult	Difficult	Easy	Very easy
Communication	Difficult	Easy	Difficult	Very easy
Production planning	Moderate	Difficult	Easy	Easy
Security	Low	Moderate	Low	High
Monitoring data	Unavailable	Moderate	Difficult	Very easy

The above figure shows the single-phase UPQC voltage swell response of the proposed system. Figure 15(a) shows voltage swell result of grid voltage, Fig. 15(b) shows the output response before applying the ADPBC in UPQC and Fig. 15(c) demonstrates the output voltage of UPQC after ADPBC technique is applied.

Figure 16 shows comparison of the UPQC controller action with various parameters such as execution time, steady state error, switching loss, and THD. From the simulation results, the comparison was mentioned in Fig. 16. The results prove that ADPBC-based controller provides the better response overshoot than a conventional controller like PI, FUZZY and ANFIS.

The hardware prototype of the proposed UPQC topology with the determinations appears in Fig. 17. The essential side or high-voltage side switches are acknowledged by IGBTs and MOSFETs are utilized for the auxiliary side or low-voltage-side switches. Programmable System-on-Chip (PSoC) is used to create the required PWM signals for the changes and to alter the terminating edge of UPQC given the detected output voltage and current.

Table 1 shows the analysis performed, the proposed ADPBC technique has been evaluated with various parameters and has produced accuracy results with all factors power quality improvement systems.

5. Conclusion

In this work, an UPQC custom control device has been used for the improvement of power quality. The choice of an UPQC device depends on the type of load connected, supply configuration at PCC and its economics. This work made an attempt to obtain the real-time performance of UPQC using adaptive distributed power balance controller in MATLAB environment. It is observed that the operation of ADPBC controller has less peak overshoot, less THD and less steady-state error, it also has a faster response than other conventional techniques. In this work, an ADPBC-based UPQC controller was proposed for compensating the PQ problem. The simulation begins with giving better nature of frameworks with low harmonic attributes. The proposed technique has accomplished low THD 7.02% in three-phase system and 4.96% in single-phase system. The proposed controller can achieve a

better performance of PQ issues compared with the FLC, PI and ANFIS-based controllers.

Int. J. Wavelets Multiresolut Inf. Process. Downloaded from www.worldscientific.com by UNIVERSITY OF NEW ENGLAND on 01/01/20. Re-use and distribution is strictly not permitted, except for Open Access articles.

References

1. S. R. Arya and K. Kant, Power quality improvement in isolated distributed generating system using DSTATCOM, *IEEE Trans. Ind. Appl.* **51**(6) (2015) 4766–4774.
2. S. R. Arya and R. Niwas, Power quality improvement in isolated distributed power generating system using DSTATCOM, *2014 IEEE Ind. Appl. Soc. Annual Meeting* (2014) 1–8.
3. M. Basu, S. P. Das and G. K. Dubey, Investigation on the performance of UPQC-Q for voltage sag mitigation and power quality improvement at a critical load point, *IET Gener. Trans. Distrib.* **2**(3) (2008) 414–423.
4. S. Chennai and Benchouia, Unified power quality conditioner based on a three-level NPC inverter using fuzzy control technique for all voltage disturbances compensation, *M. T. Front Energy* **8** (2014) 221.
5. S. K. Dash and P. K. Ray, DS1103 real-time operation and control of photovoltaic fed unified power quality conditioner, *2016 IEEE Region 10 Conf. (TENCON)* (Singapore, 2016), pp. 3424–3428.
6. S. Ivanov, M. Ciontu, D. Sacerdotianu and A. Radu (2017). Simple control strategies of the active filters within a unified power quality conditioner (UPQC), 1–4, doi:10.1109/MPS.2017.7974465.
7. J. Jayachandran and Sachithanandam, Performance investigation of artificial intelligent based controller for phase four leg shunt active filter, *R. M. Front. Energy* **9** (2015) 446.
8. S. Y. Kamble, Unified power quality conditioner for power quality improvement with advanced control strategy, *2013 Int. Mutli-Conf. Automation, Computing, Communication, Control and Compressed Sensing (iMac4s)*, 2013, pp. 432–437.
9. T. Koroglu, M. Cuma, A. Tan, M. Inci, T. Demirdelen, K. Bayindir and M. Tumay, Performance evaluation of a new hybrid unified power quality conditioner, *IEEE 6th Int. Symp. Power Electronics for Distributed Generation Systems* (2015).
10. T. Koroglu, M. U. Cuma, A. Tan, M. Inci, T. Demirdelen, K. C. Bayindir and M. Tumay, Performance evaluation of a new hybrid unified power quality conditioner (HUPQC), *2015 IEEE 6th Int. Symp. Power Electronics for Distributed Generation Systems (PEDG)* (Aachen, Germany, 2015), pp. 1–6.
11. K. H. Kuan, K. T. Tan, P. L. so and K. H. Kwan, An unified power quality conditioner for load sharing and power quality improvement, *2012 Asia-Pacific Symp. Electromagnetic Compatibility* (Singapore, 2012), pp. 963–967.
12. A. S. Kumar, S. Rajasekar and P. Ajay-D-Vimal Raj, Power Quality Profile Enhancement of Utility connected Microgrid System using ANFIS-UPQC, *SMART GRID Technologies* **29** (2015) 112–119.
13. A. S. Kumar, K. Poongothai, S. Selvakumar, M. Silambarasan and P. Ajay-D-Vimal Raj, Mitigation of Harmonic Distortion in Microgrid System using Adaptive Neural Learning Algorithm based Shunt Active Power Filter, *SMART GRID Technologies*, August 6–8 (2015), pp. 147–154.
14. C. Kumar and M. K. Mishra, LCL filter based UPQC configuration for power quality improvement, *2016 IEEE Power and Energy Society General Meeting (PESGM)* (Boston, MA, USA, 2016), pp. 1–5.
15. A. Luo *et al.*, Overview of power quality analysis and control Technology for the smart grid, Power system. *Clean Energy* **4** (2016) 1.

Int. J. Wavelets Multiresolut Inf. Process. Downloaded from www.worldscientific.com
by UNIVERSITY OF NEW ENGLAND on 01/01/20. Re-use and distribution is strictly not permitted, except for Open Access articles.

16. R. A. Modesto, S. A. Oliveira da Silva and A. Azauri da Oliveira Júnior, "Power quality improvement using a dual unified power quality conditioner/uninterruptible power supply in three-phase four-wire systems," *IET Power Electron.* **8**(9) (2015) 1595–1605.
17. B. S. Mohammed, K. S. RamaRao and P. A/L. Nallagownden, Improvement of power quality of a two feeder system using Unified Power Quality Conditioner, *2011 National Postgraduate Conf.* (Kuala Lumpur, Malaysia, 2011), pp. 1–6.
18. M. Nandhini and M. Indhumathi, Three phase four wire unified power quality conditioner for power quality improvement, *Int. J. Adv. Res.* **5** (2017) 1656–1661, doi:10.21474/IJAR01/3675.
19. R. K. Patjoshi and K. Mahapatra, High-performance unified power quality conditioner using command generator tracker-based direct adaptive control strategy, *IET Power Electronics* **9**(6) (2016) 1267–1278.
20. R. Saravanan and P. S. Manoharan, Neuro Fuzzy based unified power quality conditioner for power quality improvement Fed Induction Motor Drive, *IAES Int. J. Artif. Intell. (IJ-AI)* **4**(1) 2015, 1 ∼ 7 ISSN: 2252-8938.
21. P. Sivaperumal and S. S. Dash, Enhancement of power quality problem in grid using custom power devices, in *Proc. 2nd Int. Conf. Intelligent Computing and Applications*, eds. P. Deiva Sundari, S. Dash, S. Das and B. Panigrahi, Advances in Intelligent Systems and Computing, Vol. 467 (Springer, Singapore, 2017), pp. 367–375.
22. A. Teke, L. Saribulut and M. Tumay, A novel reference signal generation method for power quality improvement of unified power quality conditioner *IEEE Transaction on Power Delivery* **26**(4) (2011) 2205–2214.
23. Q.-N. Trinh and H.-H. Lee, Improvement of unified power quality conditioner performance with enhanced resonant control stratergy, *IET Gener. Transm. Distrib.* **8**(12) (2014) 2114–2123.
24. S. Vinnakoti and V. R. Kota, Implementation of artificial neural network based controller for a five-level converter based UPQC, *Alexandria Engineering Journal* **57**(3) (2017) 1475–1488.
25. S. Vijayasamundiswary and J. Baskaran, A novel approach to nine switch unified power quality conditioner for power quality improvement, *Int. Conf. Innovative Research In Electrical Sciences (IICIRES)* (Nagapattinam, India, 2017), pp. 1–5.